

Atmospheric aerosol, gases and meteorological parameters measured during the LAPSE-RATE campaign by Finnish Meteorological Institute and Kansas State University

David Brus¹, Jani Gustafsson¹, Osku Kemppinen^{2,†}, Gijs de Boer^{3,4}, and Anne Hirsikko¹

¹Finnish Meteorological Institute, Erik Palménin aukio 1, P.O. Box 503, FIN-00100 Helsinki, Finland

²Kansas State University, Department of Physics, 1228 N. 17th St., 66506, Manhattan, Kansas, USA

³University of Colorado, Cooperative Institute for Research in Environmental Sciences, 216 UCB, 80309, Boulder, Colorado, USA

⁴National Oceanic and Atmospheric Administration, Physical Sciences Laboratory, 325 Broadway, 80305, Boulder, Colorado, USA

[†]Currently at University of Maryland, Earth Systems Science Interdisciplinary Center, 5825 University Research Ct suite 4001, College Park, MD 20740

Correspondence: David Brus (david.brus@fmi.fi)

Abstract. Small Unmanned Aerial Systems (sUAS) are becoming very popular as affordable and reliable observation platforms. The Lower Atmospheric Process Studies at Elevation - a Remotely-piloted Aircraft Team Experiment (LAPSE-RATE), conducted in the San Luis Valley (SLV) of Colorado (USA) between July 14th - 20th, 2018, gathered together numerous sUAS, remote sensing equipment and ground based instrumentation. Flight teams from the Finnish Meteorological Institute (FMI) 5 and the Kansas State University (KSU) co-operated during LAPSE-RATE to measure and investigate the properties of aerosol particles and gases at the surface and in the lower atmosphere. During LAPSE-RATE the deployed instrumentation operated reliably, resulting in an observational dataset described below in detail. Our observations included aerosol particle number concentrations and size distributions, concentrations of CO₂ and water vapor, and meteorological parameters.

All data sets have been uploaded to the Zenodo LAPSE-RATE community archive (<https://zenodo.org/communities/lapse-rate/>).
10 The dataset DOIs for FMI airborne measurements and surface measurements are available here:
<https://doi.org/10.5281/zenodo.3993996>, Brus et al. (2020a), and for KSU airborne measurements and surface measurements are available here: <https://doi.org/10.5281/zenodo.3736772>, Brus et al. (2020b).

1 Introduction

The concentration of aerosol particles released from primary sources or formed by gas-liquid conversion and various trace gases 15 characterize the air quality worldwide. At the same time, planetary boundary layer (PBL) mixing height and lower atmospheric wind speed and direction are influenced by a variety of factors (e.g. solar and surface stored energy and terrain inhomogeneity, Carbone et al. (2010)). Removal of aerosol particles and gases from the atmosphere depends mostly on dispersion rates, transport, deposition and other atmospheric dynamical properties (Tunved et al., 2013). To understand the formation and removal of particles and gases, it is therefore necessary to measure their properties and the atmospheric conditions supporting

20 those properties throughout the vertical profile. In-situ observation of PBL properties are obtained through various techniques, including balloon soundings, tethersondes, dropsondes and hot-air balloons (e.g. Laakso et al., 2007; Greenberg et al., 2009; Nygård et al., 2017), towers (e.g. Heintzenberg et al., 2011; Andreae et al., 2015), and recently, by Unmanned Aerial Systems (UASs) (e.g. Ramanathan et al., 2007; Jonassen et al., 2015; Kral et al., 2018; Nolan et al., 2018; Barbieri et al., 2019; de Boer et al., 2020a; Girdwood et al., 2020; Harrison et al., 2021; Jensen et al., 2021; Pinto et al., 2021; Wenta et al., 2021).

25 Land-air interactions, including influences of continental, inhomogeneous terrain on lower atmospheric thermodynamic and kinematic states and the vertical distribution of aerosol and gas properties, were investigated during LAPSE-RATE field campaign. LAPSE-RATE took place in the greater SLV, Colorado between July 14th-20th, 2018. The campaign was organized in conjunction with the 6th Conference of the International Society for Atmospheric Research using Remotely-piloted Aircraft (ISARRA, de Boer et al., 2020a). Daily operational plans were developed and executed to observe several atmospheric phenomena, including boundary layer evolution during morning hours, the diurnal cycle of valley flows, convective initiation, and the properties of gases and aerosol particles (de Boer et al., 2020b). LAPSE-RATE flights were conducted under both Federal Aviation Administration (FAA) Certificates of Authorization (COAs) and FAA Part 107, with the COAs allowing maximum flight altitudes of 914 m above the ground level (AGL). In addition to the airborne assets, a variety of ground-based observational assets were deployed (see de Boer et al., 2020b, 2021; Bell et al., 2021, for details). The FMI-KSU flight team consisted 30 of two operators from the FMI and one operator from the KSU. The main objective of FMI-KSU team during the LAPSE-RATE was to provide the physical characterization of aerosol properties in vertical column, except on July 19th when the team joined the common effort to focus on cold-air drainage flows that set up during the night-time.

40 In general, there was very little known about the background aerosol concentrations within the SLV from the literature. The aerosol and generally any air quality measurements are very sparse in Colorado and are mostly concentrated around larger cities. However, a variety of primary and secondary aerosol particle sources in the SLV, including agriculture, the Great Sand Dunes National Park, wildfires, biogenic emissions, and large-scale advection of particles from the deserts and mountainous regions of the Western United States, made this an interesting location to characterize aerosol properties and their variability. Coupled with the substantial summer diurnal cycles in atmospheric temperature, humidity, turbulence and thermodynamic mixing, as well as the frequent occurrence of thunderstorms in the mountains surrounding the SLV, aerosol properties were 45 found to vary over the course of the week, as documented in Brus et al. (2021). Routine lower-atmospheric profiling allowed our team to document particle sizes and concentrations, including the occurrence of new particle formation (NPF) events , and the connection of these phenomena to boundary layer and synoptic wind regimes.

2 Description of Platforms, Modules and Sensors

50 The FMI team deployed two rotorcraft (FMI-PRKL1 and FMI-PRKL2) during LAPSE-RATE. Both rotorcraft were custom-built around the Tarot X6 hexacopter frame, which was 960 mm in diameter (rotor-to-rotor). The maximum endurance of these rotorcraft was about 15 min using 22.2V, 16000 mAh rechargeable lithium polymer (LiPo) batteries. The maximum take-off weight for these rotorcraft was 11 kg. Flights were carried out using a 3DR Pixhawk PX4 flight controller with the

55 Ardupilot software, in a manual (stabilized) mode for FMI-PRK1 and loiter (GPS position fix) mode for FMI-PRKL2. The same propulsion system, consisting of 340 kV brushless motors, 40A Electronic Speed Controllers and 18 inch (5.5 inch pitch) carbon fiber propellers, was used for both rotorcraft. The rotorcraft's setup allowed for lifting approximately 2 kg of active payload (i.e. scientific instrumentation). The overview of FMI-KSU team instrumentation and their operational characteristics are summarized in Table 1.

56 The first rotorcraft (FMI-PRKL1) was equipped with a particle measurement module consisting of two condensational particle counters (CPC, model 3007, TSI Corp.), a factory-calibrated optical particle counter (OPC, model N2, Alphasense) and a meteorological Arduino breakout (Bosch BME280, P, T and RH). Each CPC sampled at frequency of 1Hz and was adjusted at FMI to a different cut-off diameter, 7 and 14 nm, respectively. Such a configuration allows for the observation of freshly nucleated particles in a diameter range of 7 to 14 nm (see e.g. Altstädter et al., 2015, 2018) . The voltage applied to a thermal electric device (TED) of the CPC corresponds directly to the temperature difference between the saturator and condenser and determines how fast particles grow to CPC detectable sizes. The TED values of 2000 and 1000 mV were used 60 for CPC1 and CPC2, respectively, during the campaign. Each of the CPCs used a 30 cm inlet made of conductive tubing, led from the sides upwards to the top centre of the rotorcraft, where both lines were merged to an additional 10 cm piece of conductive inlet tubing, also facing upwards and ending about 10cm above propeller's plane. Penetration for such an inlet was estimated to be between 90% and 99% for particles with a diameter between 7 and 100 nm and 99 % for particles with a diameter between 100 nm and 1 μ m. The OPC-N2 was sampling with 0.5 Hz in 16 size bins with mid-bin diameters of 0.46, 65 0.66, 0.92, 1.19, 1.47, 1.83, 2.54, 3.5, 4.5, 5.75, 7.25, 9, 11, 13, 15 and 16.75 μ m. The particle module was covered from all 70 sides except the bottom with a polylactide (PLA) foam cover (2.5 cm thick) to shade the sensors from direct sun and keep the particle module thermally stable. The BME280 sensor sampled with 1 Hz, it was located below the particle module and was shielded from solar radiation, but not forcefully aspirated.

75 The second rotorcraft (FMI-PRKL2) was equipped with a gas module, consisting of a flow-through CO₂ concentration sensor (Carbocap model GMP343, Vaisala Inc.), a CO₂ and water vapor analyzer (model Li-840A, Li-Cor Environmental) and a sensor for measuring concentrations of CO, NO₂, SO₂, and O₃ (model AQT400, Vaisala Inc.). A meteorological Arduino breakout (Bosch BME280) was used to measure P, T and RH. The BME280 sensor was mounted identically to the BME280 on the FMI-PRKL1. Unfortunately, we were not able to acquire vertical profiles nor the ground level concentrations of gases with the Vaisala AQT400 sensor during LAPSE-RATE. All recorded concentrations of gases (NO₂, O₃, CO and SO₂) were far 80 below the manufacturer declared detection limits, that is why no data set for the Vaisala AQT400 sensor is provided.

85 Both CO₂ sensors were forcefully-aspirated using micro-blowers configured as air pumps (Murata, model MZB1001T02) connected to the exhaust of the sensors with flow rate of 0.6 L.min⁻¹. A Gelman filter (1 μ m filter assembly, Li-Cor Environmental) was placed in the sample airstream in front of both CO₂ sensors to avoid contamination of the optical path. The sampling frequencies of GMP343, Li-804A and BME280 were 0.5, 1 and 1 Hz, respectively.

86 A third FMI module was operated on the ground. It consisted of a condensational particle counter (CPC, model 3007, TSI Corp.), an optical particle counter (OPC, model N2, Alphasense) and a TriSonica Mini Weather Station (Applied Technologies, Inc.). Both OPCs N2, in the particle and ground module, were used with no additional inlet, as those OPCs were not meant to

be used with any kind of inlet due to the use of a fan for aerosol intake. The surface sensor module was covered from all sides with PLA foam (2.5 cm thick) to shade the sensors from direct sun and keep the particle module thermally stable. The surface
90 module was placed on the roof top of a car at about 2 m from the ground, the TriSonica Mini was mounted on a 45 cm long carbon fiber tube on top of the surface sensor module, i.e. about 2.75 m from the ground. The data of all sensors included in surface module were saved at 1 minute resolution.

Data of both FMI rotorcraft and the FMI surface sensor module were logged separately to embedded Raspberry Pi 3+ minicomputers using Python scripts to produce ASCII comma separated files, which were later converted to NetCDF format.

95 The KSU used a DJI Matrice 600 Pro rotorcraft without any modifications beyond the payload attachments, with the aircraft controlled with the Matrice 600 Pro remote controller. Both DJI TB47S (6x4500 mAh, 22.2 V) and DJI TB48S (6x5700 mAh, 22.8 V) rechargeable lithium polymer batteries were used, alternating between flights. The maximum gross take-off weight recommended by the manufacturer is 15.5 kg resulting in a maximum payload capacity of roughly 5.5 kg. The Matrice 600 Pro of KSU was equipped with an portable optical particle spectrometer (POPS, Handix Scientific LLC) measuring in the diameter
100 size range of 0.13-3 μm in 16 size bins with mid-bin diameters: 0.138, 0.151, 0.166, 0.183, 0.200, 0.219, 0.250, 0.297, 0.399, 0.534, 0.802, 1.15, 1.47, 1.893, 2.506 and 3.26 μm . During LAPSE-RATE the POPS used a horizontally oriented naked inlet approximately 9 cm (3.5 in.) long with an inner diameter of 1.7 mm (0.069 in.). POPS included electronics, and logged data to an onboard microSD card with frequency of 1 Hz. POPS was attached to the top surface of the rotorcraft body with Velcro tape. It was not shielded from direct sunlight during the flights, but was kept in shade while on the ground. A duplicate POPS
105 instrument was operated as a ground reference it was located approximately 1.8 m AGL. and used a vertically oriented tube inlet of approximately 45 cm (18 in.) long with an inner diameter of 3.175 mm (0.125 in.). The penetration through the inlet was estimated to be \sim 92% for particles with diameter of 3 μm and better for smaller ones.

3 Description of measurement location, flight strategies and completed sampling

As mentioned above, the San Luis Valley provided a variety of aerosol particle sources, sinks and processing modes. In
110 combination, the variability resulting from this processing made the San Luis Valley an interesting place to study aerosol properties and their spatial and temporal variability. One of the main sources of income for San Luis Valley inhabitants comes from farming and ranching. The primary crops grown here include potatoes, alfalfa, native hay, barley, wheat, quinoa and vegetables like lettuce, spinach, and carrots. Crops are irrigated by surface flooding water but mainly by center pivot sprinklers. Uncultivated land is often covered with low brush such as rabbitbrush, greasewood and other woody species. The land is
115 also heavily used for grazing (U.S. Fish and Wildlife Service, 2015) and references therein. The soils of the SLV are generally coarse, gravelly, sandy soils or loam, and derived mainly from volcanic rocks (Lapham, 1912).

The FMI-KSU team operated from one location throughout the entire LAPSE-RATE campaign. This location was situated along County Road 53, approximately 15 km north from Leach Airport (37°54'32.94" N, 106°2'6.83" W, 2291 m MSL), see Fig. 1. The location was flat and treeless, surrounded by grazing farmlands and generally very quiet. Occasionally the site
120 experienced emissions and aerosol production from the operation of local farm trucks. The FMI team was permitted to operate

to a maximum altitude of 914 m AGL under a FAA COA, however the aircraft was only flown to a maximum altitude of 893 m AGL. All flights operated by the KSU team were conducted up to a maximum altitude of 121 m AGL, the maximum altitude permitted under FAA Part 107.

During July 15th-18th the FMI –KSU team conducted missions focusing on profiling of aerosol particle and gas properties. In 125 total, the FMI team completed 38 vertical profile flights: 14 flights with the particle module and 24 flights with the gas module (see Table 2). The KSU team completed a total of 33 flights with their payload, including 40 individual vertical profiles. It should be noted that some of these KSU profiles were redundant, made within a few minutes of each other, and repeated in the exact same location as another profile. These redundant flights were completed to test the instrument consistency. It was found that POPS was counting consistently during vertical sampling. But during the horizontal transects, when the POPS inlet was 130 facing the direction of flight, we found fluctuations in POPS measured sample flow rate. Only vertical profile data are included in the dataset. The FMI flight strategy was to conduct only vertical flights and reach as high an altitude as possible in very short time. FMI ascent rates were between 5-8 and 3-5 m.s⁻¹ and descent rates were about 2-5 and 2-3 m s⁻¹ for flights with the particle module (FMI-PRKL1) and gas module (FMI-PRKL2), respectively. Vertical profiling was performed in cycles by alternating flights with the aircraft carrying the FMI particle module, the FMI gas module and the KSU platform, with about 135 30 minutes in between flights (please see Table 2 for details on timing, frequency and achieved altitude of all flights). The FMI surface module and KSU surface POPS were logging continuously during the time periods of flight operations (see Table 3 for details).

On the last day of FMI-KSU operations during LAPSE-RATE (July 19th), the team joined the common effort to evaluate cold-air drainage from local valleys during the morning hours. The operation started about 11:45 UTC (5:45 a.m. local time) 140 with vertical profiles every 30 min lasting about 5 hours. Only the FMI-PRKL2 and KSU rotorcraft took part in these cold-air drainage flights in an alternating fashion. For these flights ascent and descent rates were reduced to about 2 m s⁻¹ given that the target maximum altitude during these flights only extended to 350 m AGL.

4 Data Processing and Quality Control

Data files generated by the FMI particle module (FMI-PRKL1) were formatted in NetCDF format and were named according 145 to the general naming convention for the LAPSE-RATE files (FMI.PRKL1.a1.yyyy.mm.dd.hh.mm.ss.cdf), as outlined in de Boer et al. (2020b). Missing data in the dataset are marked as -9999.9. These files include the Raspberry Pi RTC time stamp, aircraft location (GPS latitude and longitude in degrees and altitude in MSL meters), basic meteorology, including temperature (°C), pressure (hPa) and relative humidity (%). Finally, these files include the total particle concentration measured by the pair 150 of CPCs (model 3007, TSI Inc.). As a reminder, these two CPCs had different cut-off diameters (D_{50}) at 7 and 14 nm (the lower size boundaries), with the upper boundary particle size more than 1 μm . The CPC calibration was done in the same way as described in Hämeri et al. (2002); the uncertainty of D_{50} values was determined to be ± 0.8 nm. The total count was compared to a desktop, full-sized, more precise CPC (model 3772, TSI Corp.) with an accuracy of about 20%, when the ambient air was sampled.

NetCDF files created from the measurements of the OPC-N2 particle counter were saved separately under the file name
155 FMI.PRKL1OPC-N2.a1.yyyy.mm.dd.hh.mm.ss.cdf. These files include the time stamp, aircraft location (GPS latitude and
longitude in degrees and altitude in meters, total aerosol number concentration in cm^{-3} and total aerosol volumetric concen-
tration in $\mu\text{m}^3 \cdot \text{cm}^{-3}$, both in a size range of 0.38-17 μm). Also included are particle number concentrations (cm^{-3}) in each bin,
including measurements in 16 size bins with mid-bin diameters of 0.46, 0.66, 0.92, 1.19, 1.47, 1.83, 2.54, 3.5, 4.5, 5.75, 7.25, 9,
11, 13, 15 and 16.75 μm , the calculated $dN/d\log D_p$ (cm^{-3}) values in each size bin, and measured PM1, PM2.5 and PM10 mass
160 concentrations in $\mu\text{g} \cdot \text{m}^{-3}$, respectively. The positioning data were provided in the files as they were measured, meteorological
parameters were cleaned off outliers and no corrections were applied, particle concentrations were cleaned of extremely high
peaks caused by vehicle emissions.

The FMI gas module dataset (FMI.PRKL2.a1.yyyy.mm.dd.hh.mm.ss.cdf) includes NetCDF files , missing data in the dataset
are marked as -9999.9. These files include the Raspberry Pi RTC time stamp, aircraft location (GPS latitude and longitude in
165 degrees, and aircraft altitude in MSL meters), and basic meteorology including temperature in degrees $^{\circ}\text{C}$, pressure in hPa
and relative humidity in %. Additionally, for both aircraft FMI-PRKL1 and FMI-PRKL2 identically, included in these data
files are aircraft attitude data (pitch, roll, yaw and heading in degrees, GPS ground speed in m s^{-1} and vertical ascent rate,
also in m s^{-1}). The attitude data are published as they were recorded without any corrections. Also included are the measured
170 CO_2 concentration in parts per million (ppm) and dew point temperature in $^{\circ}\text{C}$ as measured by Licor Li-840A. The CO_2 con-
centrations measured by the Licor Li-840A are internally compensated for water vapor concentration, pressure changes and
atmospheric temperature (for details please see the Licor Li-840A Instruction manual). Data from the Vaisala GMP343 sensor
175 were compensated for pressure, temperature, RH (obtained from the BME280 sensor) and oxygen in post-processing by using
the proprietary compensation algorithm provided by Vaisala. Even though, the BME280 sensor showed a bias of about +2
 $^{\circ}\text{C}$ in temperature, -12% in RH and +2 hPa in pressure during the LAPSE-RATE inter-comparison measurements (Barbieri et
180 al., 2019), the bias impact on compensation was minimal, less than 1%. Even when accounting for the maximum error in T,
RH and P, the resulting change (increase) in CO_2 concentration was only 2 ppm. Furthermore, both CO_2 sensors were cali-
brated in the laboratory before and after LAPSE-RATE and showed no drift in calibration. The sensors were calibrated against
standard carbon dioxide gases (traceable to WMO CO_2 scale X2007 at the FMI) at several concentrations (zero gas and 436
ppm before the campaign, and 370, 405.4 and 440.2 ppm after the campaign). The following, laboratory-derived calibration
185 constants were applied to the data sets collected by both sensors: $\text{Licor}_{\text{new}} = 0.95785 \times \text{Licor}_{\text{measured}} + 8.66055$ with $R^2 = 0.9999$
and $\text{GMP}_{\text{new}} = 0.99878 \times \text{GMP}_{\text{compensated}} + 8.77014$ with $R^2 = 0.99999$. Please note $\text{GMP}_{\text{compensated}}$ used in the equation above
and that the Vaisala compensation algorithm is confidential. Also, both sensors were tested in the FMI lab at sea level pressure
against a calibrated, high-precision gas concentration analyzer (Picarro model G2401, Picarro, Inc.) at ambient CO_2 concen-
tration. The GMP343 data were biased on average -3.4 (± 1.3) ppm and the Licor 0.3 (± 1.1) ppm. The dew point measurement
185 from the Licor LI-840A was calibrated against a DewMaster Chilled Mirror Hygrometer (Edgetech Instruments Inc.).

Measurements collected by the FMI ground module (NetCDF file names FMI.GROUNDTRISONICA-CPC.a1.
185 yyyymmdd.hhmmss.cdf) include the Raspberry Pi RTC time stamp, wind speed (m.s^{-1}), wind direction (deg), temperature ($^{\circ}\text{C}$),
relative humidity (%), and pressure (hPa) measured by the Trisonica mini weather station. Also saved is the total aerosol num-

ber concentration (cm^{-3}) measured by CPC (model 3007, TSI Inc.). The second ground module dataset (FMI.GROUNDOPC-N2.a1.yyyymmdd.hhmmss.cdf) includes the Raspberry Pi RTC time stamp, total aerosol number concentration (cm^{-3}), total aerosol volumetric concentration ($\mu\text{m}^3 \cdot \text{cm}^{-3}$) in a size range of 0.38–17 μm . Also included are the particle number concentrations in each bin (16 size bins), calculated $dN/d\log D_p$ (cm^{-3}) values in each bin (16 size bins), and the measured PM1, PM2.5 and PM10 mass concentrations ($\mu\text{g} \cdot \text{m}^{-3}$) respectively. Missing data in both of these datasets are marked as -9999.9.

The KSU airborne dataset (KSU.M600POPS.a1.yyyymmdd.hhmmss.cdf) includes the POPS internal RTC time stamp, aircraft location (GPS altitude (m MSL), altitude (m AGL), latitude and longitude (deg)), total aerosol particle count and total aerosol particle concentration (cm^{-3}) in the size range 0.13–3 μm . Also included are atmospheric pressure (hPa), internal air flow ($\text{cm}^3 \cdot \text{s}^{-1}$), counts per bin (16 size bins) and calculated $dN/d\log D_p$ (cm^{-3}) values in each bin (16 size bins).

Additionally, the KSU ground dataset (KSU.SURFACEPOPS.a1.yyyymmdd.hhmmss.cdf) includes POPS internal RTC time stamp, total aerosol particle count in the diameter size range 0.13–3 μm , total aerosol particle concentration (cm^{-3}) in the diameter size range 0.13–3 μm , pressure (hPa), internal air flow ($\text{cm}^3 \cdot \text{s}^{-1}$), counts per bin (16 size bins) and calculated $dN/d\log D_p$ (cm^{-3}) values in each bin (16 size bins with mid-bin diameters: 0.138, 0.151, 0.166, 0.183, 0.200, 0.219, 0.250, 0.297, 0.399, 0.534, 0.802, 1.15, 1.47, 1.893, 2.506 and 3.26 μm). The datasets were cleaned off the outliers and extremely high particle concentrations caused by vehicle emissions, no additional corrections were applied to data.

4.1 Dataset remarks

Throughout the collected data set, there were occasional peaks in detected aerosol number concentration caused by farm vehicles passing our sampling location. Some of these peaks resulted in particle counts up to 40 000 cm^{-3} from the CPC and up to 16 000 cm^{-3} from the POPS. These peaks typically lasted approximately 3 minutes, and were removed from the datasets. Also, a short inter-comparison (about 5 minutes) was performed before each flight among the surface and airborne particle counters to check their performance. Based on data post-processing, the CPCs of particle and surface modules compared well within the manuscript stated uncertainty of 10%, except for July 16th when NPF at the surface level took place. This is due to different calibrated cut-off diameter of each CPC. The OPCs compared within factor of 2, however it has to be considered that very low particle concentrations were measured, about 2 cm^{-3} in the OPCs size range. There were no inter-comparison measurements made for POPS instruments. For more details please see Supplementary Materials of Brus et al. (2021), where the detailed analysis was provided.

Since hysteresis in T and RH profiles collected by both FMI aircraft was noticeable, we recommend to use only data from the ascending portion of the flown profiles. The ascent data copied quite well the T and RH slopes, when compared to balloon sounding profiles made from Leach Airport. The descent data were found rather flat.

Data from the Vaisala GMP343 probe suffer from an inaccurate pressure compensation algorithm provided by Vaisala. As mentioned above, the GMP343 performed well at the sea level, however the bias increased with elevation. Therefore, we recommend use of Licor-840A data over those from the Vaisala GMP343 probe.

The merged data sets on meteorology, aerosol and gases concentrations are presented in Fig. 2 and Fig. 3 for airborne and surface measurements respectively.

5 Data Availability

Data sets collected by the FMI and the KSU during LAPSE-RATE were published together under the LAPSE-RATE community at Zenodo open data repository. For data collected using the platforms outlined in this paper, the airborne data sets of FMI-PRKL1, FMI-PRKL2 and the FMI surface module data sets can be all found here: <https://doi.org/10.5281/zenodo.3993996>, Brus et al. (2020a). The airborne data sets of KSU M600 and KSU surface data sets can be found both here: <https://doi.org/10.5281/zenodo.3736772>, Brus et al. (2020b).

All data sets have undergone quality control and false readings were eliminated. All files are available in netCDF format for each individual UAS flight and the surface data sets are available as separate daily files.

6 Summary

This publication summarizes measurements collected and data sets generated by the FMI and KSU teams during LAPSE-RATE. LAPSE-RATE took place in the San Luis Valley of Colorado during the summer of 2018. In section 2, we provided an overview of the rotorcraft deployed by these teams during this campaign, and offer insight into the types of payloads that were deployed. In Section 3 we described the teams' scientific goals and flight strategies while section 4 provides a glimpse at the data sets obtained, including a description of the measurement validation techniques applied. Section 5 provided information on data sets availability. The dataset was divided into two parts: FMI dataset containing 60 files (21 MB) and KSU dataset containing 31 files (11.3 MB), all files are available in netCDF format. To our knowledge, the data collected by these flights represent some of the only known profiles of aerosol properties collected over the San Luis Valley.

While the overall data set is limited in temporal and spatial coverage, these measurements offer unique insight into the vertical structure and diurnal variability of atmospheric thermodynamic, aerosol and gas parameters in a new location. Such observations would be difficult to obtain with other profiling methods (such as ground-based remote-sensing instrumentation). The temporal frequency and spatial extent covered by these profiles is unique to data collected using unmanned aircraft systems. This data set offers a nice example of how these systems can help to inform our general understanding of these parameters, which can be very important to understanding weather and climate.

A description of the vertical structure of key parameters as observed during LAPSE-RATE was provided in Brus et al. (2021), e.g. it includes analysis and discussion on acquired parameters and provides insight, however limited, on new particle formation events occurring over the San Luis Valley.

Author contributions. D.B. and G.B. planned and coordinated FMI missions during LAPSE-RATE campaign, D.B. conducted particle module measurements, processed, analyzed and QC FMI dataset, wrote the manuscript. J.G. provided technical support during the campaign, conducted measurements with gas module. A.H. wrote the manuscript and QC FMI dataset. O.K. conducted all KSU flights. G.B. and D.B. prepared and QC KSU dataset. All authors edited the manuscript.

Competing interests. The authors declare no conflict of interest.

Acknowledgements. The authors would like to acknowledge the following financial support of this effort: KONE foundation, ACTRIS-2 -
255 the European Union's Horizon 2020 research and innovation programme under grant agreement (No 654109), ACTRIS PPP - the European
Commission under the Horizon 2020 – Research and Innovation Framework Programme, H2020-INFRADEV-2016-2017 (Grant Agreement
number: 739530), Academy of Finland Center of Excellence programme (grant no. 307331) and the US National Science Foundation CA-
REER program (1665456). In addition, limited general support for LAPSE-RATE was provided by the US National Science Foundation (AGS
260 1807199) and the US Department of Energy (DE-SC0018985) in the form of travel support for early career participants. Support for
the planning and execution of the campaign was provided by the NOAA Physical Sciences Laboratory and NOAA UAS Program Office.
Finally, the support of UAS Colorado and local government agencies (Alamosa County, Saguache County) was critical in securing site permissions
and other local logistics. D.B. and J.G. would like to especially acknowledge Dave L. Coach for acting as a Pilot-In-Command for
the FMI team. Handix Scientific, LLC is acknowledged for providing their POPS instruments for the campaign at no cost.

References

265 Altstädter, B., Platis, A., Wehner, B., Scholtz, A., Wildmann, N., Hermann, M., Käthner, R., Baars, H., Bange, J., and Lampert, A.: ALADINA – an unmanned research aircraft for observing vertical and horizontal distributions of ultrafine particles within the atmospheric boundary layer, *Atmos. Meas. Tech.*, 8, 1627– 1639, <https://doi.org/10.5194/amt-8-1627-2015>, 2015.

Altstädter, B., Platis, A., Jähn, M., Baars, H., Lütterath, J., Held, A., Lampert, A., Bange, J., Hermann, M. and Wehner, B.: Airborne observations of newly formed boundary layer aerosol particles under cloudy conditions, *Atmos. Chem. Phys.*, 18(11), 8249–8264, doi:10.5194/acp-18-8249-2018, 2018.

270 Andreae, M. O., Acevedo, O. C., Araújo, A., Artaxo, P., Barbosa, C. G. G., Barbosa, H. M. J., Brito, J., Carbone, S., Chi, X., Cintra, B. B. L., da Silva, N. F., Dias, N. L., Dias-Júnior, C. Q., Ditas, F., Ditz, R., Godoi, A. F. L., Godoi, R. H. M., Heimann, M., Hoffmann, T., Kesselmeier, J., Könemann, T., Krüger, M. L., Lavric, J. V., Manzi, A. O., Lopes, A. P., Martins, D. L., Mikhailov, E. F., Moran-Zuloaga, D., Nelson, B. W., Nölscher, A. C., Santos Nogueira, D., Piedade, M. T. F., Pöhlker, C., Pöschl, U., Quesada, C. A., Rizzo, L. V., Ro, C.-U., Ruckteschler, N., Sá, L. D. A., de Oliveira Sá, M., Sales, C. B., dos Santos, R. M. N., Saturno, J., Schöngart, J., Sörgel, M., de Souza, C. M., de Souza, R. A. F., Su, H., Targhetta, N., Tóta, J., Trebs, I., Trumbore, S., van Eijck, A., Walter, D., Wang, Z., Weber, B., Williams, J., Winderlich, J., Wittmann, F., Wolff, S., and Yáñez-Serrano, A. M.: The Amazon Tall Tower Observatory (ATTO): overview of pilot measurements on ecosystem ecology, meteorology, trace gases, and aerosols, *Atmos. Chem. Phys.*, 15, 10723–10776, <https://doi.org/10.5194/acp-15-10723-2015>, 2015.

275 280 Barbieri, L.; Kral, S.T.; Bailey, S.C.C.; Frazier, A.E.; Jacob, J.D.; Reuder, J.; Brus, D.; Chilson, P.B.; Crick, C.; Detweiler, C.; Doddi, A.; Elston, J.; Foroutan, H.; González-Rocha, J.; Greene, B.R.; Guzman, M.I.; Houston, A.L.; Islam, A.; Kemppinen, O.; Lawrence, D.; Pillar-Little, E.A.; Ross, S.D.; Sama, M.P.; Schmale, D.G.; Schuyler, T.J.; Shankar, A.; Smith, S.W.; Waugh, S.; Dixon, C.; Borenstein, S.; de Boer, G.: Intercomparison of Small Unmanned Aircraft System (sUAS) Measurements for Atmospheric Science during the LAPSE-RATE Campaign. *Sensors*, 19, 2179, 2019.

285 Bell, T. M., Klein, P. M., Lundquist, J. K., and Waugh, S.: Remote-sensing and radiosonde datasets collected in the San Luis Valley during the LAPSE-RATE campaign, *Earth Syst. Sci. Data*, 13, 1041–1051, <https://doi.org/10.5194/essd-13-1041-2021>, 2021.

Brus, D., Gustafsson J., Kemppinen O., de Boer G., and Hirsikko A.: Atmospheric aerosol, gases and meteorological parameters measured during the LAPSE-RATE campaign - Finnish Meteorological Institute data sets [Data set]. Zenodo. <http://doi.org/10.5281/zenodo.3993996>, 2020a.

290 Brus D., Gustafsson J., Kemppinen O., de Boer G., and Hirsikko A.: Atmospheric aerosol, gases and meteorological parameters measured during the LAPSE-RATE campaign - Kansas State University data sets [Data set]. Zenodo. <http://doi.org/10.5281/zenodo.3736772>, 2020b.

Brus, D., Gustafsson, J., Vakkari, V., Kemppinen, O., de Boer, G., and Hirsikko, A.: Measurement report: Properties of aerosol and gases in the vertical profile during the LAPSE-RATE campaign, *Atmos. Chem. Phys.*, 21, 517–533, <https://doi.org/10.5194/acp-21-517-2021>, 2021.

295 Carbone, C., Decesari, S., Mircea, M., Giulianelli, L., Finessi, E., Rinaldi, M., S. Fuzzi, Marinoni, A., Duchi, R., Perrino, C., Sargolini, T., Vardè, M., Sprovieri, F., Gobbi, G. P., Angelini, F., Facchini, M.C.: Size-resolved aerosol chemical composition over the Italian Peninsula during typical summer and winter conditions. *Atmospheric Environment* 44, 5269–5278, 2010.

de Boer, G., C. Diehl, J. Jacob, A. Houston, S.W. Smith, P. Chilson, D.G. Schmale III, J. Intrieri, J. Pinto, J. Elston, D. Brus, O. Kemppinen, A. Clark, D. Lawrence, S.C.C. Bailey, M.P. Sama, A. Frazier, C. Crick, V. Natalie, E. Pillar-Little, P. Klein, S. Waugh, J.K. Lundquist, 300 L. Barbieri, S.T. Kral, A.A. Jensen, C. Dixon, S. Borenstein, D. Hesselius, K. Human, P. Hall, B. Argrow, T. Thornberry, R. Wright

and J.T. Kelly: Development of community, capabilities and understanding through unmanned aircraft-based atmospheric research: The LAPSE-RATE campaign, *Bull. Amer. Meteor. Soc.*, 101(5), E684-E699, <https://doi.org/10.1175/BAMS-D-19-0050.1>, 2020a.

de Boer, G., A. Houston, J. Jacob, P. Chilson, S. Smith, B. Argrow, D. Lawrence, J. Elston, D. Brus, O. Kempinen, P. Klein, J. Lundquist, S. Waugh, S. Bailey, A. Frazier, M. Sama, C. Crick, D. Schmale III, J. Pinto, E. Pillar-Little, V. Natalie, A. Jensen: Data Generated During 305 the 2018 LAPSE-RATE Campaign: An Introduction and Overview, *Earth Syst. Sci. Data*, 12, 3357–3366, <https://doi.org/10.5194/essd-12-3357-2020>, 2020b.

de Boer, G., Waugh, S., Erwin, A., Borenstein, S., Dixon, C., Shanti, W., Houston, A., and Argrow, B.: Measurements from mobile surface vehicles during the Lower Atmospheric Profiling Studies at Elevation – a Remotely-piloted Aircraft Team Experiment (LAPSE-RATE) , 310 *Earth Syst. Sci. Data*, 13, 155–169, <https://doi.org/10.5194/essd-13-155-2021>, 2021.

Girdwood, J., Smith, H., Stanley, W., Ulanowski, Z., Stopford, C., Chemel, C., Doulgeris, K.-M., Brus, D., Campbell, D., and Mackenzie, R.: Design and field campaign validation of a multi-rotor unmanned aerial vehicle and optical particle counter, *Atmos. Meas. Tech.*, 13, 315 6613–6630, <https://doi.org/10.5194/amt-13-6613-2020>, 2020.

Greenberg, J.P., Guenther, A.B., Turnipseed, A.: Tethered balloon-based soundings of ozone, aerosols, and solar radiation near Mexico City during MIRAGE-MEX, *Atmospheric Environment*, 43, 16, p. 2672, <https://doi.org/10.1016/j.atmosenv.2009.02.019>, 2009.

Hämeri, K., Koponen, I.K., Aalto, P.P. and Kulmala, M: The particle detection efficiency of the TSI-3007 condensation particle counter, *J. Aer. Sci.*, 33, 10, [https://doi.org/10.1016/S0021-8502\(02\)00090-3](https://doi.org/10.1016/S0021-8502(02)00090-3), 2002.

Harrison, R. G., Nicoll, K. A., Tilley, D. J., Marlton, G. J., Chindea, S., Dingley, G. P., Iravani, P., Cleaver, D. J., du Bois, J. L., and Brus, D.: Demonstration of a Remotely Piloted Atmospheric Measurement and Charge Release Platform for Geoengineering, *Journal of Atmospheric and Oceanic Technology*, 38(1), 63-75, 2021.

Heintzenberg, J., Birmili, W., Otto, R., Andreae, M. O., Mayer, J.-C., Chi, X., and Panov, A.: Aerosol particle number size distributions and particulate light absorption at the ZOTTO tall tower (Siberia), 2006–2009, *Atmos. Chem. Phys.*, 11, 8703-8719, 320 <https://doi.org/10.5194/acp-11-8703-2011>, 2011.

Jensen, A. A., Pinto, J. O., Bailey, S. C. C., Sobash, R. A., de Boer, G., Houston, A. L., Chilson, P. B., Bell, T., Romine, G., Smith, S. W., Lawrence, D. A., Dixon, C., Lundquist, J. K., Jacob, J. D., Elston, J., Waugh, S., and Steiner, M., Assimilation of a Coordinated Fleet 325 of Uncrewed Aircraft System Observations in Complex Terrain: EnKF System Design and Preliminary Assessment. *Monthly Weather Review* 149, 5, 1459-1480, doi:10.1175/MWR-D-20-0359.1, 2021.

Jonassen, M. O., Tisler, P., Altstädter, B., Scholtz, A., Vihma, T., Lampert, A., König-Langlo, G., Lüpkes, C.: Application of remotely piloted aircraft systems in observing the atmospheric boundary layer over Antarctic sea ice in winter. *Polar Res.* 34: 25651, doi: 10.3402/polar.v34.25651, 2015.

Kral, S.T.; Reuder, J.; Vihma, T.; Suomi, I.; O'Connor, E.; Kouznetsov, R.; Wrenger, B.; Rautenberg, A.; Urbancic, G.; Jonassen, M.O.; Båserud, L.; Maronga, B.; Mayer, S.; Lorenz, T.; Holtslag, A.A.M.; Steeneveld, G.-J.; Seidl, A.; Müller, M.; Lindenberg, C.; Langohr, C.; Voss, H.; Bange, J.; Hundhausen, M.; Hilsheimer, P.; Schygulla, M.: Innovative Strategies for Observations in the Arctic Atmospheric Boundary Layer (ISOBAR)—The Hailuoto 2017 Campaign. *Atmosphere*, 9, 268, 2018.

Laakso, L., Grönholm, T., Kulmala, L., Haapanala, S., Hirsikko, A., Lovejoy, E.R., Kazil, J., Kurtén, T., Boy, M., Nilsson, E.D., Sogachev, A., 335 Riipinen, I., Stratmann, F., Kulmala, M.: Hot-air balloon as a platform for boundary layer profile measurements during particle formation. *Boreal Environment Research* 12, 279–294, 2007.

Lapham M. H.: Soils of the San Luis Valley, U. S. Department of Agriculture, Bureau of Soil Circular No. 52, 1912.

Nolan, P.J., Pinto, J., González-Rocha, J., Jensen, A., Vezzi, C.N., Bailey, S.C.C., De Boer, G., Diehl, C., Laurence, R., III, Powers, C.W., Foroutan, H., Ross, S.D., Schmale, D.G., III.: Coordinated Unmanned Aircraft System (UAS) and Ground-Based Weather Measurements
340 to Predict Lagrangian Coherent Structures (LCSs). *Sensors*, 18, 4448. <https://doi.org/10.3390/s18124448>, 2018.

Nygård, T., Tisler, P., Vihma, T., Pirazzini, R., Palo, T. and Kouznetsov, R.: Properties and temporal variability of summertime temperature inversions over Dronning Maud Land, Antarctica. *Q.J.R. Meteorol. Soc.*, 143: 582-595. doi:10.1002/qj.2951, 2017.

Pinto, J. O., Jensen, A. A., Jiménez, P. A., Hertneky, T., Muñoz-Esparza, D., Dumont, A., and Steiner, M.: Real-time WRF large-eddy simulations to support uncrewed aircraft system (UAS) flight planning and operations during 2018 LAPSE-RATE, *Earth Syst. Sci. Data*,
345 13, 697–711, <https://doi.org/10.5194/essd-13-697-2021>, 2021.

Ramanathan, V.; Ramana, M.V.; Roberts, G.; Kim, D.; Corrigan, C.; Chung, C.; Winker, D. Warming trends in Asia amplified by brown cloud solar absorption. *Nature*, 448, 575, 2007.

Tunved, P., Ström, J., and Krejci, R.: Arctic aerosol life cycle: linking aerosol size distributions observed between 2000 and 2010 with air mass transport and precipitation at Zeppelin station, Ny-Ålesund, Svalbard, *Atmos. Chem. Phys.*, 13, 3643-3660, [https://doi.org/10.5194/acp-13-3643-2013](https://doi.org/10.5194/acp-350-13-3643-2013), 2013.

U.S. Fish and Wildlife Service. Land protection plan for the San Luis Valley Conservation Area. Lakewood, CO: U.S. Department of the Interior, U.S. Fish and Wildlife Service. 151 p., 2015.

Wenta, M., Brus, D., Doulgeris, K., Vakkari, V., and Herman, A.: Winter atmospheric boundary layer observations over sea ice in the coastal zone of the Bay of Bothnia (Baltic Sea), *Earth Syst. Sci. Data*, 13, 33–42, <https://doi.org/10.5194/essd-13-33-2021>, 2021.

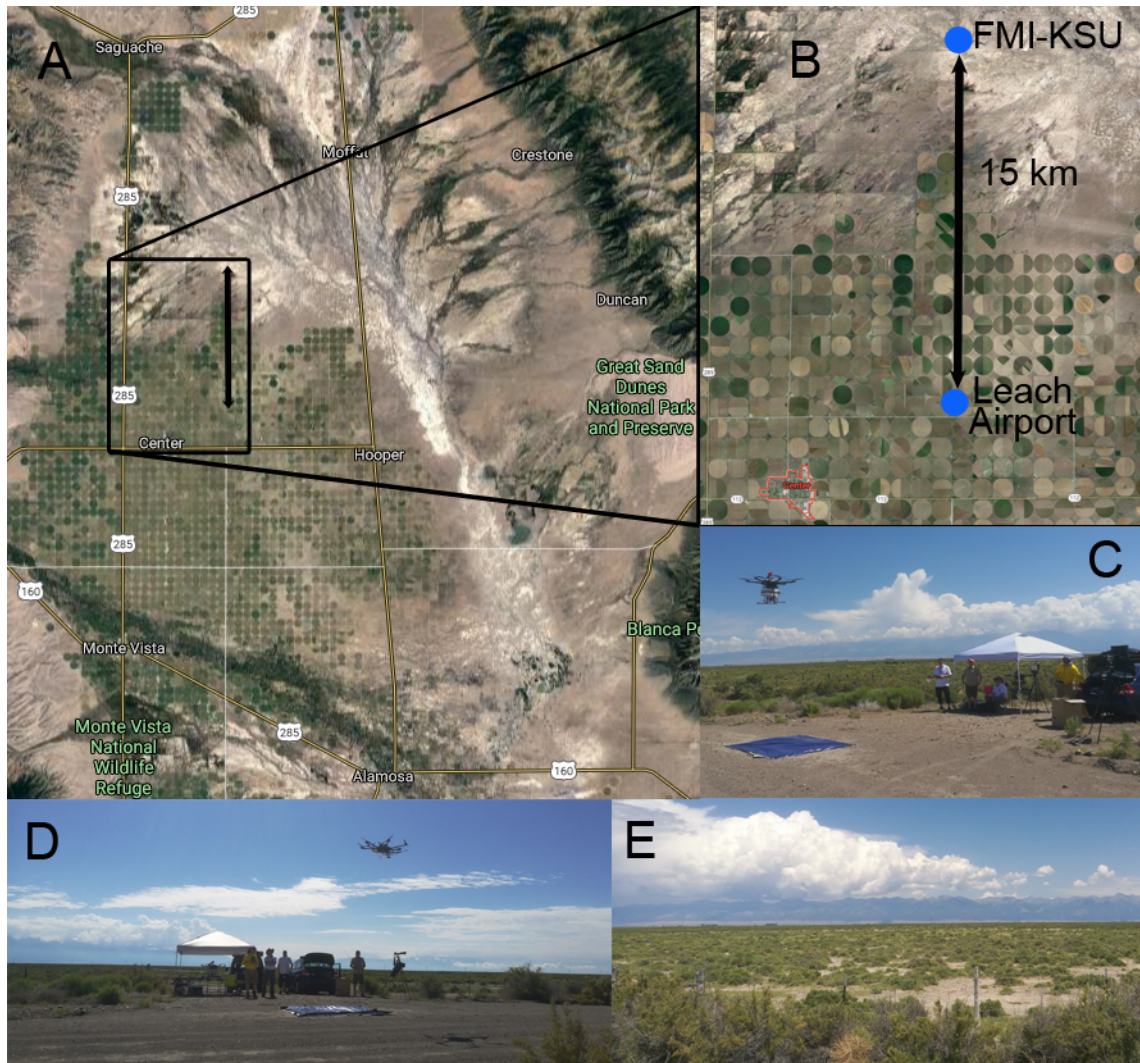


Figure 1. A) Map of wider San Luis Valley, CO, B) map cutout of FMI-KSU team location - 15 km north of Leach airport, located approximately 3.2 km ENE of the commercial district of Center, Colorado and 32 km NNW of Alamosa, Colorado. ©Google Maps C) FMI-KSU team operation spot NE view, D) FMI-KSU team operation spot view towards E, E) view of typical surroundings of FMI-KSU team spot.

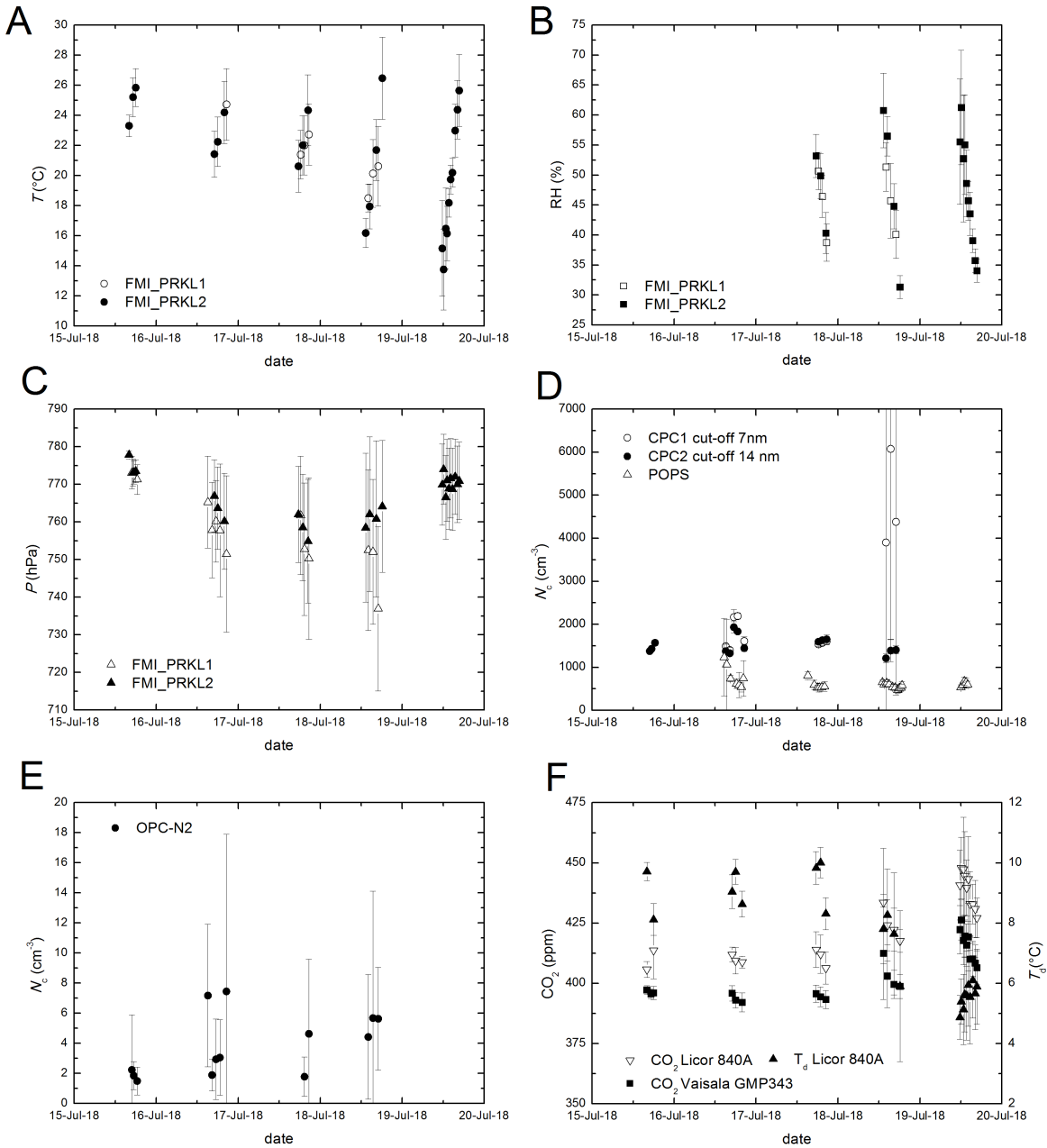


Figure 2. Overview of data collected in vertical profile, mean values with standard deviations as error-bars: A) temperature, B) relative humidity, C) pressure, D) total aerosol number concentration by CPCs and POPPS (0.13–3 μ m), note the elevated concentration measured by CPC1 characterizing the event, E) aerosol number concentration by OPC-N2 (0.3–18 μ m) and F) CO_2 concentration by Licor Li-840A and Vaisala GMP343 and dew point temperature by Licor Li-840A.

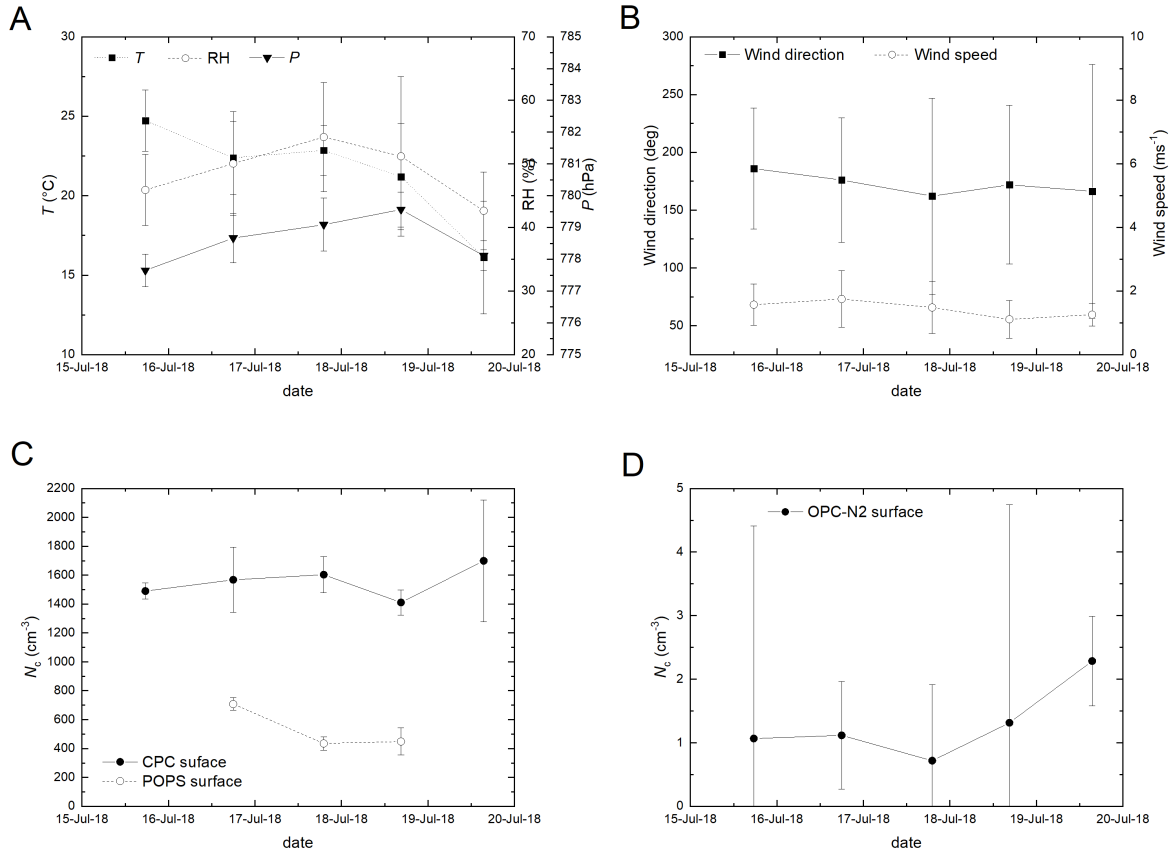


Figure 3. Overview of data collected with the FMI surface module placed on car roof about 2.75 m AGL, mean values with standard deviations as error-bars: A) temperature, relative humidity, pressure, B) wind direction and speed by Trisonica mini weather station C) total aerosol number concentration by CPC and POPS (0.13–3 μ m, placed about 1.8 m AGL), and D) aerosol number concentration by OPC-N2 (0.3–18 μ m)

Table 1. An overview of sensors and their operational characteristics provided by manufacturer . The sensor use in airborne and/or ground based measurements is specified in sensor name column as mission: a-airborne, g-ground based

Sensor	Resolution	Accuracy	Range	Flow rate	Response time
CPC, TSI 3007 Particle conc. (cm ⁻³) mission: a & g			0-10 ⁵ cm ⁻³ , Diameter: 0.01->1 µm	0.7 L.min ⁻¹	1 s
OPC, Alphasense N2 Particle conc. (cm ⁻³) mission: a & g			0-10 ⁴ part.s ⁻¹ , Diameter: 0.38-17 µm at 16 bins	1.2 L.min ⁻¹	1 s
BME280 T (°C) RH (%) Pressure (hPa) mission: a & g	0.01 <0.01 0.18 Pa	±0.5 °C ±3 % ±1 hPa	-40-85 °C 0-100 % 300-1100 hPa		1 s 1 s 6 ms
GMP343, Vaisala CO ₂ (ppm) mission: a	14-bits	±3ppm +1% of reading	0-1000 ppm	0.6 L.m ⁻¹	2s
Li-840A, Licor CO ₂ (ppm) T _d (°C) mission: a	14-bits across user-specified range 14-bits across user-specified range	<1.5% of reading <1.5% of reading	0-20000 ppm -25-45 °C, RH: 0 to 95% RH Non-Condensing	0.6 L.m ⁻¹ 0.6 L.m ⁻¹	1s 1s
TriSonica Mini WS, Applied Tech. T (°C) RH (%) Pressure (hPa) Wind speed (m.s ⁻¹) Wind direction (deg.) mission: g	0.1 0.1 1 0.1 1	±2°C ±3% ±10 hPa ±0.1 m.s ⁻¹ ±1 deg.	-25-80 °C 0-100 % 500-1150 hPa 0-30 m.s ⁻¹ x/y: 0-360 deg., z: ±30 deg.		1 s 1 s 1 s 1 s 1 s
POPS, Handix Sci. Particle conc. (cm ⁻³) mission: a & g		±10% <1000 cm ⁻³ at 0.1 L.m ⁻¹	0-1250 cm ⁻³ , Diameter: 0.13 – 3 µm at 16 bins	0.18 L.min ⁻¹	1 s

Table 2. UAS vertical profile measurements - an overview of platforms, missions, flight times and achieved altitudes.

platform	mission	date	start time (UTC)	end time (UTC)	altitude (m MSL)	altitude (m AGL)
FMI-PRKL1	aerosols/meteo	15/07/18	16:51:49	16:56:55	2483.49	175.49
			17:24:40	17:32:00	2436.60	128.60
			18:24:54	18:33:12	2449.68	141.68
		16/07/18	15:06:47	15:14:55	2819.67	511.67
			16:20:53	16:29:21	2823.44	515.44
			17:30:33	17:41:14	2730.81	422.81
			18:37:31	17:47:36	2949.73	641.73
			20:33:20	20:42:56	2994.55	686.55
		17/07/18	18:17:18	18:26:03	2924.22	616.22
			19:24:35	19:35:13	2992.33	684.33
			20:41:37	20:53:53	3119.02	811.02
		18/07/18	14:03:55	14:14:33	3155.00	847.00
			15:26:03	15:36:27	3028.59	720.59
			16:59:06	17:05:55	3201.53	893.53
FMI-PRKL2	gases/meteo	15/07/18	16:02:28	16:06:28	2356.88	48.88
			17:12:39	17:17:13	2441.78	133.78
			17:59:24	18:05:11	2409.02	101.02
		16/07/18	17:00:44	17:08:28	2675.27	367.27
			18:00:08	18:08:55	2703.60	395.60
			19:57:24	20:06:33	2781.37	473.37
		17/07/18	17:37:19	17:46:52	2773.00	465.00
			18:53:43	19:02:34	2814.49	506.49
			20:27:20	20:36:53	2910.11	602.11
		18/07/18	13:19:00	13:31:21	2971.37	663.37
			14:29:00	14:44:16	3004.27	696.27
			16:25:00	16:40:26	3013.40	705.40
			18:10:00	18:24:36	2912.85	604.85
		19/07/18	11:44:33	11:53:42	2669.10	361.10
			12:07:00	12:24:09	2658.34	350.34
			12:46:00	12:53:43	2667.16	359.16
			13:08:00	13:19:10	2666.06	358.06
			13:41:00	13:49:25	2667.75	359.75
			14:11:00	14:22:36	2669.65	361.65
			14:42:00	14:55:43	2664.22	356.22
			15:30:00	15:45:19	2657.98	349.98
			16:12:00	16:22:25	2658.15	350.15
			16:42:00	16:53:32	2663.10	355.10

platform	mission	date	start time (UTC)	end time (UTC)	altitude (m MSL)	altitude (m AGL)
KSU POPS	aerosols	16/07/18	14:40:46	14:49:51	2401.3	125.4
			15:23:44	15:37:17	2419.4	142.4
			16:32:25	16:41:06	2410.6	126.6
			18:17:44	18:24:58	2416.7	126.4
			19:01:43	19:09:54	2333.0	39.4
			19:43:41	19:47:18	2354.6	52.1
			20:17:20	20:22:46	2429.7	126.8
		17/07/18	15:10:38	15:24:49	2401.3	125.7
			17:02:14	17:09:42	2401.6	129.0
			17:58:12	18:04:40	2403.5	127.5
			18:29:15	18:40:16	2379.9	100.0
			19:15:14	19:26:11	2417.7	131.3
			20:03:59	20:09:49	2424.7	127.4
		18/07/18	12:59:49	13:04:27	2397.5	127.4
			13:31:21	13:42:29	2398.4	127.2
			14:16:06	14:22:23	2400.8	131.3
			14:58:05	15:02:03	2394.9	126.2
			15:59:52	16:08:59	2402.2	127.2
			16:44:06	16:46:37	2408.2	128.2
			17:30:21	17:38:37	2408.4	126.4
			17:59:11	18:03:40	2415.5	128.6
			18:29:37	18:33:06	2417.9	126.5
			18:45:25	18:49:16	2419.4	126.1
		19/07/18	12:01:01	12:05:05	2433.6	138.8
			12:28:54	12:31:35	2435.9	142.8
			12:59:42	13:02:06	2429.7	139.1
			13:29:40	13:32:18	2427.4	139.0
			13:59:47	14:02:37	2425.1	137.4

Table 3. Surface measurements at altitude 2291 m MSL - overview of platform and data coverage

platform	date	start time (UTC)	end time (UTC)
FMI surface module	15/07/18	15:34:35	19:36:35
	16/07/18	14:45:29	22:10:47
	17/07/18	17:01:53	21:08:15
	18/07/18	13:03:29	19:05:08
	19/07/18	11:37:20	16:56:36
KSU POPS surface	16/07/18	15:52:34	16:16:44
	17/07/18	18:17:46	20:31:13
	18/07/18	13:30:39	18:13:44

355 **Acronyms**

AGL above ground level. 2, 4, 5, 15

CPC condensation particle counter. 3, 5, 7, 14–16

FMI Finnish Meteorological Institute. 1–9, 13, 15, 17, 19

KSU Kansas State University. 1, 2, 8

360 **LAPSE-RATE** The Lower Atmospheric Process Studies at Elevation - a Remotely-piloted Aircraft Team Experiment. 1–6, 8,

9

MSL mean sea level. 4, 19

NPF new particle formation. 2, 7

OPC optical particle counter. 3, 6, 7, 14–16

365 **PBL** planetary boundary layer. 1

POPS portable optical particle spectrometer. 4, 5, 7, 9, 14–16, 18, 19

SLV San Luis Valley. 1, 2, 4

sUAS Small Unmanned Aerial Systems. 1